Traces of Z_2-Vortices in $CuCrO_2$, $AgCrO_2$, and $PdCrO_2$

Mamoun Hemmida, Hans-Albrecht Krug von Nidda, and Alois Loidl

Experimental Physics V, Center for Electronic Correlations and Magnetism, University of Augsburg, 86135 Augsburg, Germany

The spin-spin relaxation of the two-dimensional triangular lattice antiferromagnets $CuCrO_2$, $AgCrO_2$, and $PdCrO_2$ is investigated by electron spin resonance spectroscopy. The data proof excellent agreement with very recent predictions for the Z_2-vortex ordering scenario in triangular Heisenberg antiferromagnets derived by Okubo and Kawamura.

Currently, two-dimensional (2D) triangular lattice antiferromagnets (TAF)s are attracting a lot of attention due to remarkable magneto-electrical properties. Delafossite compounds like the insulators $CuCrO_2$ and $AgCrO_2$ exhibit a multiferroic behavior, the coexistence of magnetic order and ferroelectricity, concomitantly with a 120° spin-spiral structure.[1,2] On the other hand, metallic $PdCrO_2$ shows unusual critical phenomena in the specific heat[3] and an unconventional anomalous Hall effect[4] attributed to the local exchange between palladium conduction electrons and localized frustrated chromium spins, which undergo a 120° spin order as well. In both cases the exact microscopic mechanisms are still not resolved, but the spin chirality emerging from the geometrical frustration of the chromium spins on the triangular lattice is supposed to be a prerequisite of the observed phenomena. Thus, for deeper insight, a closer inspection of the microscopic magnetic properties of these systems is urgently required.

Previously, we have shown by means of electron spin resonance (ESR) technique that the spin relaxation in the 2D frustrated TAFs $HCrO_2$, $LiCrO_2$, and $NaCrO_2$ can be ascribed to magnetic vortices.[5] These 2D rock-salt compounds contain the same triangular chromium planes like the delafossites. They are of dominant Heisenberg character, because for Cr^{3+} with half-filled t_{2g} shell (spin $S = 3/2$) in octahedral ligand field, the anisotropy is very small. Therefore, the vortices were expected to be of Z_2-type,[6] but the temperature dependence of the corresponding correlation length $\xi(T)$ was not derived so far. Our analysis of the ESR linewidth suggested $\xi(T)$ to behave similar to the case of Berezinskii–Kosterlitz–Thouless (BKT) vortices in the XY model,[7,8] e.g., realized in the honeycomb lattices $BaNi_2P_2O_8$[9] and $BaNi_2V_2O_8$,[10] but with slight modifications reminiscent to the melting mechanism of a 2D solid treated by Halperin and Nelson,[11] and by Young (KTHNY model).[12] However, this was only empirical analogy without any theoretical confirmation. Meanwhile, the correlation length of Z_2-vortices in the Heisenberg TAF has been derived by Okubo and Kawamura indicating a modified BKT-law as well.[13] Moreover, a very recent theoretical nonequilibrium relaxation study of the anisotropic antiferromagnetic Heisenberg model on the triangular lattice reveals that the BKT critical region becomes divergently wide as the anisotropy decreases.[14] At the isotropic Heisenberg point, it shows apparent BKT criticality in a wide range of temperatures. Here we present new ESR data of the delafossite compounds $CuCrO_2$, $AgCrO_2$, and $PdCrO_2$ and discuss the impact of the latest theoretical findings on our results.

Over two decades ago, Kawamura and Miyashita (KM) studied theoretically the ordering process in the 2D Heisenberg TAF via Monte-Carlo simulations and found topological defects — so-called Z_2-vortices.[6] In contrast to the vortices considered in the 2D XY model by Berezinskii[7] and Kosterlitz and Thouless,[8] where the topological quantum number, which indicates the number of circulations of spins within the vortex, can take any integer value, Z_2-vortices are characterized by a two-valued topological quantum number, only. This type of vortex can be understood in the frame of spin chirality as follows: In a 2D Heisenberg TAF, frustration is partially released by forming a local 120° spin structure. These short-range spin correlations give rise to an additional degree of freedom called the vector chirality, i.e., left- or right-handed circulation. In this sense the Z_2-vortices are formed by the chiral vectors and characterized by a two-valued topological quantum number.[6] Like in the 2D XY model, where BKT vortices are bound in vortex–antivortex pairs below the Kosterlitz–Thouless temperature T_{KT}, one expects a topological phase transition in the 2D Heisenberg TAF at a certain temperature T_{KM}, above which the Z_2-vortices dissociate.

Only very recently, the temperature dependence of the correlation length $\xi(T)$ between the Z_2 vortices has been found to be similar to the BKT case[13,15,16]

$$\xi(T) = \xi_0 \exp \frac{b}{\tau^{\nu}} \quad \text{where} \quad \tau = \frac{T}{T_{KM}} - 1, \tag{1}$$

but with a slightly smaller value of $\nu = 0.42$ (instead of 0.5), an arbitrary b parameter, and T_{KM} substituting T_{KT} in the normalized temperature τ. At the same time the authors give an improved estimation of the transition temperature

$$T_{KM} = 0.285 \left| \frac{2J}{k_B} \right| S^2, \tag{2}$$

where J and k_B denote the exchange integral and Boltzmann constant, respectively. Here we recall that in the KTHNY model a similarly reduced value of the exponent $\nu = 0.37$ was obtained.[11,12] Concerning the experimental proof of Z_2-vortices it is important to note that these chiral fluctuations on TAFs are related to four-spin correlations, the direct experimental study of which is difficult to realize.[17] Indeed, the ESR linewidth is determined by four-spin correlation functions, which makes the dynamical

chirality or rather chiral fluctuations accessible to ESR technique. Using some approximations outlined previously[5,18,19] the linewidth ΔH is proportional to the third power of the correlation length:

$$\Delta H = \Delta H_\infty \exp\left(\frac{3b}{\tau^\nu}\right) \tag{3}$$

with ΔH_∞ being the asymptotic high-temperature value of the linewidth. This expression will be used below to evaluate the experimental data.

Polycrystalline samples of $CuCrO_2$ and $PdCrO_2$ were prepared by solid-state reaction as described in literature.[1,20] $AgCrO_2$ was prepared by solid-state reaction as well but in addition to the procedure described be Seki *et al.*[1] the stoichiometric mixture of Ag and Cr_2O_3 is heated for 48 h in O_2 at 900 °C, then pestled and heated again for 48 h in O_2 at 900 °C. Powder x-ray diffraction measurements show a single phase in $CuCrO_2$ and $PdCrO_2$ but a very small amount of impurity in $AgCrO_2$ as reported in literature.[1] Magnetization measurements have been performed using a superconducting quantum interference device (SQUID; Quantum Design MPMS5) at temperatures $2 \leq T \leq 300$ K. The ESR measurements were performed in a Bruker ELEXSYS E500-CW spectrometer at X-band (9.36 GHz) frequency equipped with a continuous He-gas flow cryostat (Oxford Instruments) working in the temperature range $4.2 \leq T \leq 300$ K. The polycrystalline samples were fixed in a quartz tube with paraffin. Due to the lock-in technique with field modulation the field derivative of the microwave-absorption signal is detected as a function of the static magnetic field. Resonance absorption occurs, if the incident microwave energy matches the energy of magnetic dipolar transitions between the electronic Zeeman levels.

For the two multiferroic TAFs $CuCrO_2$ and $AgCrO_2$, typical ESR spectra are depicted in the top and middle frames of Fig. 1, respectively. In the whole paramagnetic regime both compounds show a single exchange-narrowed resonance line, which is perfectly described by a symmetrical Lorentzian curve. In contrast, as shown in the bottom frame of Fig. 1, the resonance lines of metallic $PdCrO_2$ can be well described by an asymmetrical Lorentzian (Dysonian) curve due to the skin effect which appears in conductive compounds because of the interaction between the applied microwave field and mobile charge carriers. This yields an admixture of dispersion χ' to the absorption χ'' depending on the ratio of skin depth and sample size.[21] In the present case we found $\chi'/\chi'' \approx 0.5$. Note that for all compounds due to the large linewidth at low temperatures the counter resonance at $-H_{res}$ is included in the fit.[22]

The half width at half maximum ΔH at room temperature amounts to about 178, 205, and 224 Oe for $CuCrO_2$, $AgCrO_2$, and $PdCrO_2$, respectively. These values can be explained in terms of zero-field splitting and dipolar contributions similar to the estimates given by Angelov *et al.* for the related rock-salt compounds.[23] On decreasing temperature the spectra broaden rapidly, shift to higher resonance fields, and become undetectable on approaching the ground state at T_N. The high-temperature resonance fields of these compounds resemble a g-value of about $g = 1.98$, close to 2 indicative for the nearly quenched orbital momentum typical for Cr^{3+}.[24] The temperature

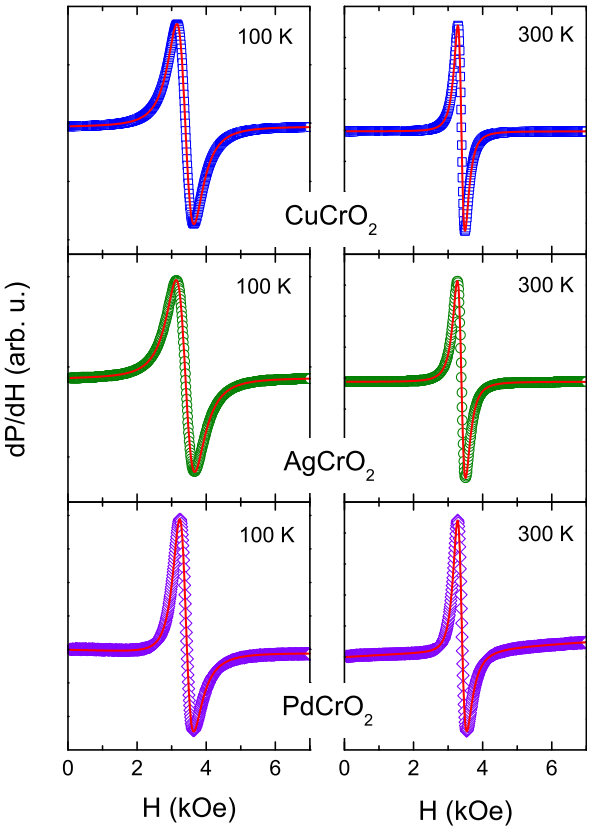

Fig. 1. (Color online) ESR spectra of $CuCrO_2$, $AgCrO_2$, and $PdCrO_2$ in X-band for selected temperatures. The solid line indicates a fit with the field derivative of a Lorentz line in $CuCrO_2$ and $AgCrO_2$ and with a Dyson line in $PdCrO_2$.

dependence of the corresponding fit parameters, i.e., intensity, resonance field, and linewidth, is depicted in Figs. 2, 3, and 4 for $CuCrO_2$, $AgCrO_2$, and $PdCrO_2$, respectively. The ESR intensities have been plotted together with the static spin susceptibilities, revealing the characteristic maximum of 2D antiferromagnets, which scales with the exchange constant J/k_B. The deviation of the ESR intensities from static spin susceptibilities at low temperatures is similar to that observed in the geometrically frustrated spinel compound $ZnCr_2O_4$, where it has been attributed to the increasing influence of nonresonant relaxational modes with strongly increasing linewidth.[25]

Based on our previous results in rock salts[5,26] and the recent theoretical achievements[13] we fitted the linewidth data by eq. (3) setting $\nu = 0.37$ (KTHNY-model) and $\nu = 0.42$ (KM-model), respectively, and taking ΔH_∞, b, and T_{KM}, as fit parameters. Table I summarizes the corresponding results. Note that the melting temperature T_m substitutes T_{KM} in the reduced temperature τ, when using the KTHNY model. As one can see, the linewidth data of all three compounds are very well described by both exponents in the whole temperature range without adding any residual linewidth contribution. This is in very good agreement with the theoretically predicted wide BKT critical regime.[14] Only in $PdCrO_2$ slight deviations show up at high temperatures which probably reflect additional relaxation contributions due to the mobile charge carriers.

Looking closer to the results, it is evident that the R^2 values slightly prefer the lower exponent $\nu = 0.37$. In

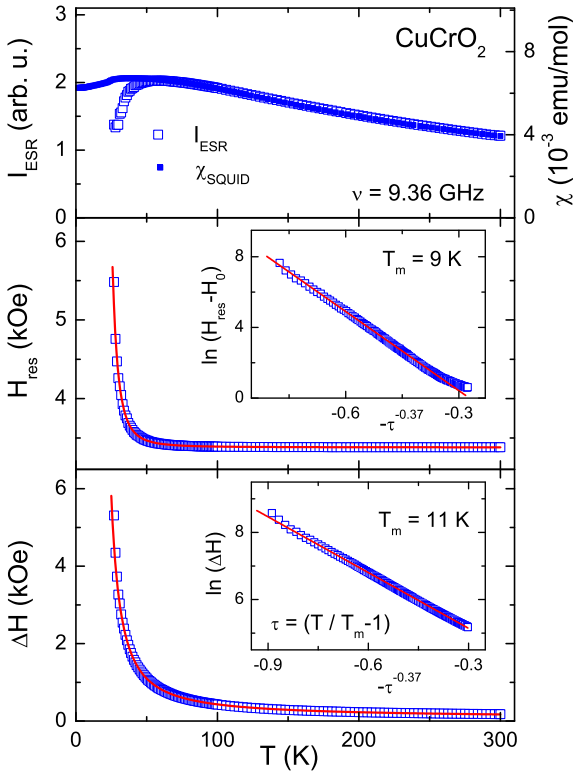

Fig. 2. (Color online) Temperature dependence of the intensity with SQUID susceptibility, resonance field, and linewidth in $CuCrO_2$. The fit (solid line) is described in the text. Insets: Logarithmic plots of the resonance shift $\ln(H_{res} - H_0)$ vs $-\tau^{-0.37}$ (middle frame), and $\ln(\Delta H)$ vs $-\tau^{-0.37}$ (lower frame).

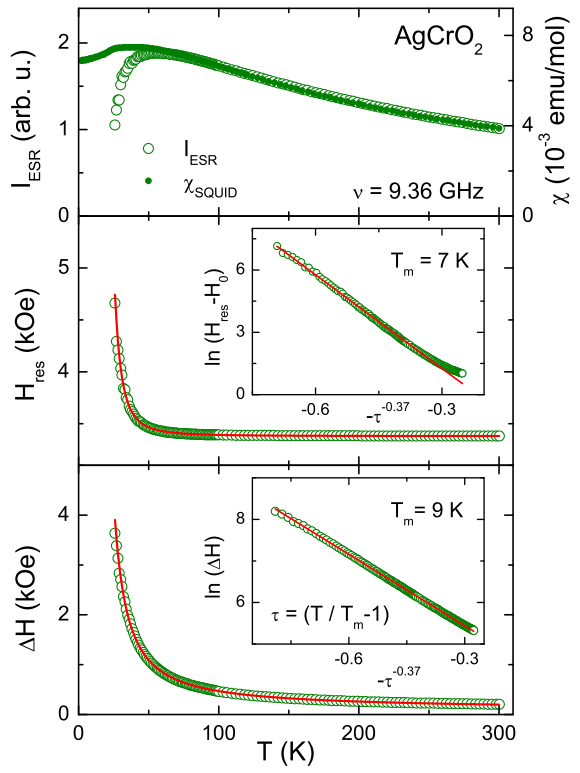

Fig. 3. (Color online) Temperature dependence of the intensity with SQUID susceptibility, resonance field, and linewidth in $AgCrO_2$. The fit (solid line) is described in the text. Insets: Logarithmic plots of $\ln(H_{res} - H_0)$ vs $-\tau^{-0.37}$ (middle frame), and $\ln(\Delta H)$ vs $-\tau^{-0.37}$ (lower frame).

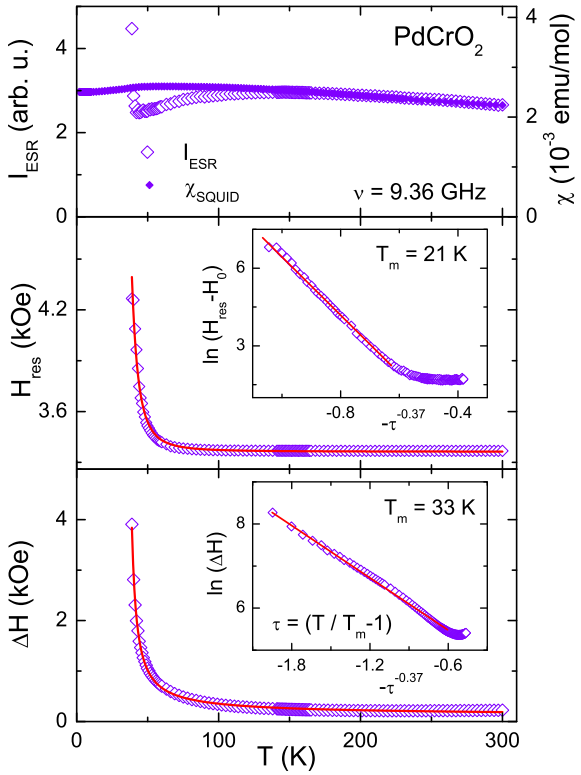

Fig. 4. (Color online) Temperature dependence of the intensity with SQUID susceptibility, resonance field, and linewidth in $PdCrO_2$. The fit (solid line) is described in the text. Insets: Logarithmic plots of $\ln(H_{res} - H_0)$ vs $-\tau^{-0.37}$ (middle frame), and $\ln(\Delta H)$ vs $-\tau^{-0.37}$ (lower frame).

addition for $CuCrO_2$ and $AgCrO_2$ the obtained melting temperature T_m comes much closer to the numerically estimated T_{KM} than that obtained from the fit with $\nu = 0.42$. In $PdCrO_2$ both approaches lead to comparable values of T_m and T_{KM}. It seems that the KTHNY model for melting of 2D solids and the KM model for TAFs yield equivalent results at least in the disordered phase. Therefore, in Figs. 2, 3, and 4, only the fit curves obtained with $\nu = 0.37$ are depicted. Moreover, the temperature dependent shift of the resonance fields with respect to the asymptotic high-temperature value H_0 is also satisfactorily described by eq. (3) using $\nu = 0.37$ in all three compounds. The resulting parameter T_m is about 20% smaller than that obtained from the linewidth in the Cu- and Ag-systems, but deviates significantly in $PdCrO_2$. However, note that no theoretical predictions of the influence of vortices on the resonance field does exist so far.

To complete the picture we have also reanalyzed the linewidth data of the rock-salt compounds $HCrO_2$, $LiCrO_2$, and $NaCrO_2$ using $\nu = 0.42$ and compared to our earlier fitting with $\nu = 0.37$. The results are given in the lower part of Table I. Again, using the exponent $\nu = 0.37$ is favorable concerning the resulting vortex-transition temperature, which comes closer to the numerical estimate of the KM model for $HCrO_2$ and $NaCrO_2$. Thus, our ESR experiments strongly indicate the presence of Z_2-vortices in the TAFs $ACrO_2$ as expected from the theory.[13] Remarkably, these findings are not constrained to the chromium oxide systems: very recent analysis of high-field ESR measurements in TAF $NiGa_2S_4$ found that the BKT scenario ($\nu = 0.5$) cannot give a reasonable description of the linewidth data in the

Table I. Delafossites: Néel temperature T_N and exchange constant J/k_B as taken from literature. T_{KM} [Theory] calculated from eq. (2). Fit parameters for the temperature dependence of the ESR linewidth corresponding to KM model and KTHNY model as described in the text. The quality of the fit is characterized by the coefficient of determination $R^2 = 1 - \sum_i (y_i - f_i)^2 / \sum_i (y_i - \bar{y})^2$, where y_i, f_i, and $\bar{y}$ denote the data, the corresponding fit values, and the total average of the data, respectively.

		$CuCrO_2$	$AgCrO_2$	$PdCrO_2$
T_N (K)[20]		24	21	37.5
J/k_B (K)[20]		−11.4	−9	−23
T_{KM} (K)	[Theory]	14.6	11.5	29.5
KM model				
ΔH_∞ (Oe)		43.4(1)	47.2(1)	88.5(1)
b		1.90(2)	2.54(4)	0.62(1)
T_{KM} (K)		10.3(1)	5.4(1)	32.7(1)
R^2		0.99974	0.99973	0.99784
KTHNY model				
ΔH_∞ (Oe)		31.6(1)	40.1(1)	73(2)
b		1.86(1)	1.93(2)	0.68(1)
T_m (K)		11.3(1)	9.0(1)	33.3(1)
R^2		0.99989	0.99985	0.99808
		$HCrO_2$	$LiCrO_2$	$NaCrO_2$
J/k_B (K)[5]		−12	−39	−20
T_{KM} (K)	[Theory]	15.4	50.0	25.7
T_{KM} (K)	[$\nu = 0.42$]	4.5(1)	58.1(1)	22.1(1)
T_m (K)	[$\nu = 0.37$]	8.4(6)	58.9(1)	23.9(1)

intermediate temperature regime $8 \leq T \leq 23$ K. Instead, a Z_2 scenario was favored.[27] This is now corroborated, because applying eq. (3) with the lower exponent values, 0.42 as well as 0.37, leads to a satisfactory fit of the data.[28]

Note that, although the reported ESR measurements are constrained to the paramagnetic regime, the presence of Z_2-vortices can be anticipated down to T_m or $T_{KM} < T_N$. This was evidenced in the case of $NaCrO_2$, where muon-spin rotation revealed a fluctuating crossover regime extending well below T_N, with a peak of the relaxation rate $1/T_1$ around $T \approx 25$ K.[29] The values of T_m or T_{KM} extracted from the ESR data nicely coincide with this relaxation peak indicating the coexistence of Z_2-vortices in the ordered regime. As spin chirality has been related to ferroelectricity as well as to the unconventional anomalous Hall effect, therefore we speculate that the Z_2-vortices may be involved into the exotic ground-state properties observed in these materials. However, the current state of experimental and theoretical studies cannot clarify this point so far.

In summary, we have discovered a universal behavior of the ESR linewidth in the temperature regime $T_N \leq T \leq 300$ K for $ACrO_2$ delafossite as well as rock-salt compounds, which can be well explained in terms of spin relaxation via Z_2-vortices. The temperature dependence of the Z_2-vortex correlation length $\xi(T)$ derived from the linewidth data agrees very well with recent theoretical predictions for 2D frustrated Heisenberg triangular lattice antiferromagnets.

Acknowledgments We are very grateful to Anna Pimenov and V. Tsurkan for sample preparation and to T. Okubo for fruitful discussions. This work supported by the Deutsche Forschungsgemeinschaft (DFG) partially within the Transregional Collaborative Research Center TRR 80 (Augsburg-Munich) and the Research Unit FOR 960.

1) S. Seki, Y. Onose, and Y. Tokura: Phys. Rev. Lett. **101** (2008) 067204.
2) K. Kimura, H. Nakamura, S. Kimura, M. Hagiwara, and T. Kimura: Phys. Rev. Lett. **103** (2009) 107201.
3) H. Takatsu, H. Yoshizawa, S. Yonezawa, and Y. Maeno: Phys. Rev. B **79** (2009) 104424.
4) H. Takatsu, S. Yonezawa, C. Michioka, K. Yoshimura, and Y. Maeno: J. Phys.: Conf. Ser. **200** (2010) 012198.
5) M. Hemmida, H.-A. Krug von Nidda, N. Büttgen, A. Loidl, L. K. Alexander, R. Nath, A. V. Mahajan, R. F. Berger, R. J. Cava, Y. Singh, and D. C. Johnston: Phys. Rev. B **80** (2009) 054406.
6) H. Kawamura and S. J. Miyashita: J. Phys. Soc. Jpn. **53** (1984) 4138.
7) V. L. Berezinskii: Sov. Phys. JETP **32** (1971) 493.
8) J. M. Kosterlitz and D. J. Thouless: J. Phys. C **6** (1973) 1181.
9) P. Gaveau, J. P. Boucher, L. P. Regnault, and Y. Henry: J. Appl. Phys. **69** (1991) 6228.
10) M. Heinrich, H.-A. Krug von Nidda, A. Loidl, N. Rogado, and R. J. Cava: Phys. Rev. Lett. **91** (2003) 137601.
11) B. I. Halperin and D. R. Nelson: Phys. Rev. Lett. **41** (1978) 121.
12) A. P. Young: Phys. Rev. B **19** (1979) 1855.
13) T. Okubo and H. Kawamura: J. Phys. Soc. Jpn. **79** (2010) 084706.
14) T. Misawa and Y. Motome: J. Phys. Soc. Jpn. **79** (2010) 073001.
15) J. M. Kosterlitz: J. Phys. C **7** (1974) 1046.
16) H. Kawamura, A. Yamamoto, and T. Okubo: J. Phys. Soc. Jpn. **79** (2010) 023701.
17) V. P. Plakhty, S. V. Maleyev, J. Kulda, J. Wosnitza, D. Visser, and E. Moskvin: Europhys. Lett. **48** (1999) 215.
18) H. Benner and J. B. Boucher: in *Magnetic Properties of Layered Transition Metal Compounds*, ed. L. J. deJongh (Kluwer, Dordrecht, 1990) p. 323.
19) J. Becker: Ph. D. thesis, TU Darmstadt, Germany (1996).
20) J. Doumerc, A. Wichainchai, A. Ammar, M. Pouchard, and P. Hagenmuller: Mater. Res. Bull. **21** (1986) 745.
21) S. E. Barnes: Adv. Phys. **30** (1981) 801.
22) J. P. Joshi and S. V. Bhat: J. Magn. Res. **168** (2004) 284.
23) S. Angelov, J. Darriet, C. Delmas, and G. Le Flem: Solid State Commun. **50** (1984) 345.
24) A. Abragam and B. Bleaney: *Electron Paramagnetic Resonance of Transtion Ions* (Clarendon, Oxford, U.K., 1970).
25) H. Martinho, N. O. Moreno, J. A. Sanjurjo, C. Rettori, A. J. Garcia-Adeva, D. L. Huber, S. B. Oseroff, W. Ratcliff, S.-W. Cheong, P. G. Pagliuso, J. L. Sarrao, and G. B. Martins: J. Appl. Phys. **89** (2001) 7050.
26) M. Hemmida, H.-A. Krug von Nidda, and A. Loidl: J. Phys.: Conf. Ser. **200** (2010) 022016.
27) H. Yamaguchi, S. Kimura, M. Hagiwara, Y. Nambu, S. Nakatsuji, Y. Maeno, A. Matsuo, and K. Kindo: J. Phys. Soc. Jpn. **79** (2010) 054710.
28) T. Okubo: private communication (2009).
29) A. Olariu, P. Mendels, F. Bert, B. G. Ueland, P. Schiffer, R. F. Berger, and R. J. Cava: Phys. Rev. Lett. **97** (2006) 167203.